Distributed Primary Frequency Control through Multi-Terminal HVDC Transmission Systems

Martin Andreasson*, Roger Wiget, Dimos V. Dimarogonas, Karl H. Johansson and Göran Andersson

***Abstract*—This paper presents a decentralized controller for sharing primary AC frequency control reserves through a multi-terminal HVDC grid. By using passivity arguments, the proposed controller is shown to stabilize the closed-loop system consisting of the interconnected AC and HVDC grids, given any positive controller gains. The static control errors resulting from the proportional controller are quantified and bounded by analyzing the equilibrium of the closed-loop system. The proposed controller is applied to a test grid consisting of three asynchronous AC areas interconnected by an HVDC grid, and its effectiveness is validated through simulation.**

I. Introduction

Transmitting power over long distances with minimal losses is one of the greatest challenges in today's power transmission systems. The strong rising share of renewables increased the distances between power generation and consumption. This is a driving factor behind long-distance power transmission. One such example are large-scale off-shore wind farms, which often require power to be transmitted in cables over long distances to the mainland power grid [4]. High-voltage direct current (HVDC) power transmission is a commonly used technology for long-distance power transmission. Its higher investment costs compared to AC transmission lines are compensated by its lower resistive losses for sufficiently long distances [15]. The break-even point, i.e., the point where the total construction and operation costs of overhead HVDC and AC lines are equal, is typically 500-800 km [16]. However, for cables, the break-even point is typically less than 50 km [18]. Increased use of HVDC for electrical power transmission suggests that future HVDC transmission systems are likely to consist of multiple terminals connected by several HVDC transmission lines [11]. Such systems are referred to as Multi-terminal HVDC (MTDC) systems in the literature. The main technical obstacle to overcome in order to realize such MTDC is the development of a DC breaker [10]. There are a few advanced ideas to realize this device in the near future [5].

Maintaining an adequate DC voltage is the single most important practical control problem for HVDC transmission systems. If the DC voltage deviates too far from the nominal operational voltage, equipment could be damaged, resulting in loss of power transmission capability and high costs.

Many existing AC transmission grids are connected through HVDC links, usually used for bulk power transfer between the AC areas. The fast operation of the DC converters however would also enable frequency regulation of one of the connected AC grids through the HVDC link. One practical example of this is the island of Gotland in Sweden, which is only connected to the main Nordic grid through an HVDC cable [3]. However, since the main Nordic AC grid has orders of magnitudes higher inertia than the AC grid of Gotland, the influence of the frequency regulation on the main grid will be negligible.

By connecting several AC grids by an MTDC system, primary frequency regulation reserves may be shared, which reduces the need for frequency regulation reserves in the individual AC systems [13]. In [8], distributed control algorithms have been applied to share primary frequency control reserves of asynchronous AC transmission systems connected through an MTDC system. However, the proposed controller requires a slack bus to control the DC voltage, defeating the purpose of distributing the primary frequency regulation reserves. In [2], [1], distributed controllers for secondary voltage control of MTDC systems are proposed, which do not rely on a slack bus. Both of the aforementioned controllers however rely on the presence of a communication network. While a communication network might already be present, it introduces the issue of time delays, due to large geographical distances in MTDC systems, and has a certain outage risk. The impacts of delays have been analyzed in [8], and have been found to seriously degrade performance and destabilize the power system. A distributed controller without the need of a slack bus is proposed in [7]. Stability is guaranteed in the absence of communication delays. However, the voltage dynamics of the HVDC system are neglected. Moreover, the implementation of the controller is not realistic, as every local controller needs to access the DC voltages of all terminals. In [9] and [17], decentralized controllers are employed to share primary frequency control reserves. In [17] no stability analysis of the closed-loop system is performed, whereas [9] guarantees stability provided that the connected AC areas have identical parameters and the voltage dynamics of the HVDC system are neglected.

Due to the inherent difficulties of time-delays, we pro-

Martin Andreasson, Dimos V. Dimarogonas and Karl H. Johansson are with the ACCESS Linnaeus Centre, KTH Royal Institute of Technology, Stockholm, Sweden. Roger Wiget and Göran Andersson are with the Power Systems Laboratory, ETH Zurich, Zurich, Switzerland. This work was supported in part by the European Commission by the Hycon2 project, the Swedish Research Council (VR) and the Knut and Alice Wallenberg Foundation. * Corresponding author. E-mail: mandreas@kth.se

pose a decentralized proportional controller for distributing primary frequency control reserves, which relies only on local measurements. The controller is shown to distribute the primary frequency control reserves between the connected AC systems, while maintaining an adequate DC voltage. In contrast to [9], we prove that the closed-loop system is globally asymptotically stable for any set of system parameters and controller gains by using passivity arguments. We also explicitly model the voltage dynamics of the MTDC system, and extend our result to AC systems consisting of multiple generators. Due to inherent properties of proportional controllers, the steady-state values of the voltages and frequencies will deviate from their reference values. We quantify these deviations by provable upper bounds.

The remainder of this paper is organized as follows. In Section II, the mathematical notation is defined. In Section III, the system model and the control objectives are defined. In Section IV, a decentralized proportional controller for distributing primary frequency control is analyzed. In Section V, the equilibrium of the closed-loop system is analyzed. In Section VI, the HVDC line model is expanded to also consider the inductances of the DC lines. In Section VII, simulations of the distributed controller on a four-terminal MTDC test system are provided, showing the effectiveness of the proposed controller. The paper ends with a discussion and concluding remarks in Section VIII.

II. Preliminaries

Let $\mathcal{G}$ be a graph. Denote by $\mathcal{V} = \{1, \dots, n\}$ the vertex set of $\mathcal{G}$, and by $\mathcal{E} = \{1, \dots, m\}$ the edge set of $\mathcal{G}$. Let $\mathcal{N}_i$ be the set of neighboring vertices to $i \in \mathcal{V}$. In this paper we will only consider static, undirected and connected graphs. For the application of control of MTDC power transmission systems, this is a reasonable assumption as long as there are no power line failures. Denote by $\mathcal{B}$ the vertex-edge incidence matrix of $\mathcal{G}$, and let $\mathcal{L}_\mathcal{W} = \mathcal{B}W\mathcal{B}^T$ be the weighted Laplacian matrix of $\mathcal{G}$, with edge-weights given by the elements of the diagonal matrix W. We denote the space of real-valued $n \times n$-valued matrices by $\mathbb{R}^{n\times m}$. Let $\mathbb{C}^-$ denote the open left half complex plane, and $\bar{\mathbb{C}}^-$ its closure. We denote by $c_{n\times m}$ a vector or matrix of dimension $n \times m$, whose elements are all equal to c. For a symmetric matrix A, $A > 0$ ($A \geq 0$) is used to denote that A is positive (semi) definite. I_n denotes the identity matrix of dimension n. For simplicity, we will often drop the notion of time dependence of variables, i.e., $x(t)$ will be denoted x for simplicity. Let $\|\cdot\|_\infty$ denote the maximal absolute value of the elements of a vector.

Definition 1. *Consider the dynamical system*

$$\begin{aligned} \dot{x} &= f(x, u) \\ y &= h(x, u). \end{aligned}$$

The above system is said to be strictly passive *if there exists a positive semidefinite function $W(x)$, and a positive definite function $\psi(x)$ such that $u^T y \geq \dot{W} + \psi(x)$. The same system is said to be* output strictly passive *if there exists a positive semidefinite function $W(x)$, and some function $\rho(y)$ such that $u^T y \geq \dot{W} + y^T\rho(y)$, and $y^T\rho(y) > 0$ for $y \neq 0$ [20], [12].*

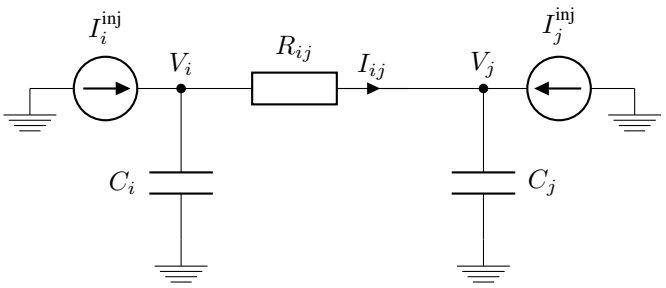

Figure 1. R-line model of a transmission line.

III. Model and problem setup

We will here give a unified model for an MTDC system interconnected with several asynchronous AC systems. We consider an MTDC transmission system consisting of n converters, each connecting to an AC system, denoted $1, \dots, n$. The converters are assumed to be connected by an MTDC transmission grid. The dynamics of converter i is assumed to be given by

$$\begin{aligned} C_i\dot{V}_i &= -\sum_{j\in\mathcal{N}_i} I_{ij} + I_i^{\text{inj}} \\ &= -\sum_{j\in\mathcal{N}_i} \frac{1}{R_{ij}}(V_i - V_j) + I_i^{\text{inj}}, \end{aligned} \tag{1}$$

where V_i is the voltage of converter i, $C_i > 0$ is its capacitance, I_i^{inj} is the injected current from an AC grid connected to the DC converter. The constant R_{ij} denotes the resistance of the HVDC transmission line connecting the converters i and j. This simple DC line model is illustrated in Figure 1. The graph corresponding to the HVDC line connections is assumed to be connected. The AC system is assumed to consist of a single generator which is connected to the corresponding DC converter, representing an aggregate model of the AC grid. The dynamics of the AC system are given by the swing equation [14]:

$$m_i\dot{\omega}_i = -K_i^{\text{droop}}(\omega_i - \omega^{\text{ref}}) + P_i^{\text{nom}} + P_i^m - P_i^{\text{inj}}, \tag{2}$$

where ω_i is the frequency of the generator, ω^{ref} is the reference frequency and $m_i > 0$ is its moment of inertia. The constant P_i^{nom} is the nominal generated power of generator i, P_i^m is the uncontrolled deviation from the nominal generated power, P_i^{inj} is the power injected to the DC system through the converter and $K_i^{\text{droop}} > 0$ is the gain of the frequency droop controller of the generator. We define $P_i^{\text{droop}} = -K_i^{\text{droop}}(\omega_i - \omega^{\text{ref}})$, and state the control objective.

Objective 1. *The primary frequency control action should be distributed fairly amongst the generators, i.e.*

$$\lim_{t\to\infty} \left| P_i^{droop}(t) + \frac{1}{n}\sum_{i=1}^{n} P_i^m \right| \leq e^{droop} \quad \forall i = 1, \dots, n,$$

where e^{droop} is a given scalar. Furthermore, the frequencies of the AC systems, as well as the converter voltages, should not deviate too far from their nominal values, i.e.

$$\lim_{t\to\infty} |V_i(t) - V_i^{ref}| \leq e^V \quad \forall i = 1,\dots,n$$
$$\lim_{t\to\infty} |\omega_i(t) - \omega^{ref}| \leq e^\omega \quad \forall i = 1,\dots,n,$$

where V_i^{ref} is the reference DC voltage of converter i, ω^{ref} is the reference frequency and e^V and e^ω are given scalars.

Remark 1. *The reference voltage V_i^{ref} will typically originate from an optimal power flow analysis, like [19], and can thus be considered constant over the short time-periods which are considered in this work.*

IV. Decentralized MTDC control

In this section we propose a decentralized controller for the frequency control of AC systems connected through an MTDC network. This controller does not rely on a single voltage regulator for the MTDC system, but the voltage regulation is distributed among all converters. The local controller governing the power injections into the MTDC network is given by

$$P_i^{\text{inj}} = P_i^{\text{inj, nom}} + K_i^\omega(\omega_i - \omega^{\text{ref}}) + K_i^V(V_i^{\text{ref}} - V_i), \quad (3)$$

where $P_i^{\text{inj, nom}}$ is the nominal injected power, and $K_i^\omega > 0$ and $K_i^V > 0$ are positive controller gains for all $i = 1,\dots,n$. The HVDC converter is assumed to be perfect and instantaneous, i.e., injected power on the AC side is immediately converted to DC power without losses. Furthermore the dynamics of the converter are ignored, implying that the converter tracks the output of controller (3) perfectly. This assumption is reasonable due to the dynamics of the converter typically being orders of magnitudes faster than the AC dynamics. The relation between the injected HVDC current and the injected AC power is thus given by

$$V_i I_i^{\text{inj}} = P_i^{\text{inj}}. \quad (4)$$

By linearizing (4) around the equilibrium where $V_i = V^{\text{nom}}$ for all $i = 1,\dots,n$, the following linear relation is obtained

$$V^{\text{nom}} I_i^{\text{inj}} = P_i^{\text{inj}}. \quad (5)$$

Combining the voltage dynamics (1), the frequency dynamics (2), the voltage controller (3) and the power-current relationship (5), we obtain the following closed-loop dynamics

$$\begin{bmatrix}\dot\omega\\ \dot V\end{bmatrix} = \underbrace{\begin{bmatrix}-M(K^\omega + K^{\text{droop}}) & MK^V\\ \frac{1}{V^{\text{nom}}}CK^\omega & -C\left(\mathcal{L}_R + \frac{K^V}{V^{\text{nom}}}\right)\end{bmatrix}}_{\triangleq A}\begin{bmatrix}\omega\\ V\end{bmatrix} + \begin{bmatrix}M\left((K^\omega + K^{\text{droop}})\omega^{\text{ref}}1_{n\times1} - K^V V^{\text{ref}}\right)\\ C\left(\frac{1}{V^{\text{nom}}}K^V V^{\text{ref}} - \frac{\omega^{\text{ref}}}{V^{\text{nom}}}K^\omega 1_{n\times1}\right)\end{bmatrix} + \begin{bmatrix}M(P^m + P^{\text{nom}} - P^{\text{inj, nom}})\\ \frac{1}{V^{\text{nom}}}CP^{\text{inj, nom}}\end{bmatrix} \quad (6)$$

where $\omega = [\omega_1,\dots,\omega_n]^T$, $V = [V_1,\dots,V_n]^T$, $M = \text{diag}({m_1}^{-1},\dots,{m_n}^{-1})$, $D = \text{diag}(d_1,\dots,d_n)$, $C = \text{diag}([C_1^{-1},\dots,C_n^{-1}])$, $K^\omega = \text{diag}([K_1^\omega,\dots,K_n^\omega])$, $K^{\text{droop}} = \text{diag}([K_1^{\text{droop}},\dots,K_n^{\text{droop}}])$, $K^V = \text{diag}([K_1^V,\dots,K_n^V])$, $P^{\text{nom}} = [P_1^{\text{nom}},\dots,P_n^{\text{nom}}]^T$, $P^{\text{inj, nom}} = [P_1^{\text{inj, nom}},\dots,P_n^{\text{inj, nom}}]^T$. $P^m = [P_1^m,\dots,P_n^m]^T$ and $\mathcal{L}_R$ is the weighted Laplacian matrix of the graph representing the HVDC transmission lines, denoted $\mathcal{G}_R$, whose edge-weights are given by the conductances $\frac{1}{R_{ij}}$. The following assumption is made on the reference frequency and reference voltages.

Assumption 1. *The point $[\omega^T, V^T]^T = [\omega^{ref}1_{1\times n}, (V^{ref})^T]^T$ is an equilibrium of (6), when $P^m = 0_{n\times1}$. By substituting this in (6), we obtain that $P^{nom} = P^{inj,\ nom}$, and $V^{nom}\mathcal{L}_R V^{ref} = P^{inj,\ nom} = P^{nom}$.*

Remark 2. *Assumption 1 implies that the reference frequency and reference voltages define an equilibrium of the closed-loop system when the deviation from the nominal power generation is zero.*

We define the incremental frequencies and voltages as

$$\hat\omega = \omega - \omega^{\text{ref}}1_{n\times1} \quad (7)$$
$$\hat V = V - V^{ref}. \quad (8)$$

By Assumption 1, the decentralized MTDC control system given by (6), can be written as

$$\begin{bmatrix}\dot{\hat\omega}\\ \dot{\hat V}\end{bmatrix} = \begin{bmatrix}-M(K^\omega + K^{\text{droop}}) & MK^V\\ \frac{1}{V^{\text{nom}}}CK^\omega & -C\left(\mathcal{L}_R + \frac{K^V}{V^{\text{nom}}}\right)\end{bmatrix}\begin{bmatrix}\hat\omega\\ \hat V\end{bmatrix} + \begin{bmatrix}MP^m\\ 0_{n\times1}\end{bmatrix}. \quad (9)$$

By decomposing (9) into two subsystems, we obtain

$$\begin{cases}\dot{\hat\omega} = -M(K^{\text{droop}} + K^\omega)\hat\omega + MK^V u_1\\ y_1 = \frac{1}{V^{\text{nom}}}K^\omega\hat\omega\end{cases} \quad (S_1)$$

$$\begin{cases}\dot{\hat V} = -C\left(\mathcal{L}_R + \frac{1}{V^{\text{nom}}}K^V\right)\hat V + Cu_2\\ y_2 = \hat V,\end{cases} \quad (S_2)$$

where (S_1) and (S_2) are interconnected through $u_1 = y_2 + (K^V)^{-1}P^m, u_2 = y_1$. The interconnection structure is shown in Figure 2. We will use passivity arguments to show that the interconnected system is asymptotically stable. First, we show that both (S_1) and (S_2) are strictly passive.

Lemma 1. *The system (S_1) is strictly passive.*

Proof: Consider the storage function

$$W_1 = \frac{1}{2V^{\text{nom}}}\hat\omega^T\left(K^\omega(K^V)^{-1}M^{-1}\right)\hat\omega.$$

Differentiating W_1 with respect to time along trajectories of

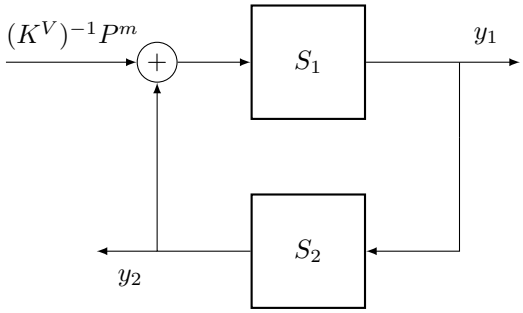

Figure 2. Block diagram of the interconnected system.

(S_1) yields

$$\begin{aligned}\dot{W}_1 &= \frac{1}{V^{\text{nom}}}\hat{\omega}^T\left(K^\omega(K^V)^{-1}M^{-1}\right)\dot{\hat{\omega}}\\ &= \frac{1}{V^{\text{nom}}}\hat{\omega}^T K^\omega(K^V)^{-1}\left(-(K^{\text{droop}}+K^\omega)\hat{\omega}+K^V u_1\right)\\ &= -\frac{1}{V^{\text{nom}}}\hat{\omega}^T K^\omega(K^V)^{-1}(K^{\text{droop}}+K^\omega)\hat{\omega}+y_1^T u_1,\end{aligned}$$

which shows that (S_1) is strictly passive. ∎

Lemma 2. *The system (S_2) is strictly passive.*

Proof: Consider the storage function

$$W_2 = \frac{1}{2}\hat{V}^T C^{-1}\hat{V}.$$

Differentiating W_2 with respect to time along trajectories of (S_2) yields

$$\begin{aligned}\dot{W}_2 &= \hat{V}^T C^{-1}\dot{\hat{V}}\\ &= \hat{V}^T\left(-\left(\mathcal{L}_R+\frac{1}{V^{\text{nom}}}K^V\right)\hat{V}+u_2\right)\\ &= -\hat{V}^T\left(\mathcal{L}_R+\frac{1}{V^{\text{nom}}}K^V\right)\hat{V}+y_2^T u_2,\end{aligned}$$

which shows that (S_2) is strictly passive. ∎

Theorem 1. *The decentralized MTDC control system given by* (9) *is globally asymptotically stable.*

Proof: The interconnection of any two strictly passive systems is asymptotically stable [12], if the input is zero. The non-zero input of (9) can be removed by introducing incremental states which are zero at the equilibrium of (9). The details of this construction are straightforward but rather tedious, and are thus omitted here and throughout the paper. Since the storage functions W_1 and W_2 are radially unbounded, the stability of (9) is global. ∎

Remark 3. *Note that although we can guarantee stability of the decentralized MTDC control system, Theorem 1 gives no further insight about the equilibrium. Nor does it guarantee that Objective 1 is fulfilled. In the following section, we will address these issues.*

V. Equilibrium analysis

We will now study the equilibrium of the globally asymptotically stable system (9). We make the following additional assumptions on the controller gains, in order to draw conclusions about the equilibrium of (9).

Assumption 2. *The controller gains satisfy $K_i^\omega = k^\omega, K_i^{droop} = k^{droop}, K_i^V = k^V\ \forall i = 1,\dots,n.$*

With the previous assumptions made, and having provided necessary stability conditions for the closed-loop system (6), we are ready to analyze its equilibrium.

Theorem 2. *Assume that Assumptions 1 and 2 hold, then Objective 1 is satisfied for the following coefficients*

$$\begin{aligned}e^{droop} &= \frac{k^{droop}}{k^\omega+k^{droop}}\left(\frac{1}{n}\left|\sum_{i=1}^n P_i^m\right|\right.\\ &\qquad\left.+\max_i|P_i^m|\left(1+\frac{1}{V^{nom}}\sum_{i=2}^n\frac{1}{\lambda_i(\mathcal{L}_R)}\right)\right)\\ e^V &= \frac{k^\omega\left|\sum_{i=1}^n P_i^m\right|}{nk^{droop}k^V}+\frac{\max_i\left|P_i^m\right|}{V^{nom}}\sum_{i=2}^n\frac{1}{\lambda_i(\mathcal{L}_R)}\\ e^\omega &= \frac{1}{k^{droop}}\left(\frac{\left|\sum_{i=1}^n P_i^m\right|}{n}\right.\\ &\qquad\left.+\max_i P_i^m\left(1+\frac{k^V}{V^{nom}}\sum_{i=2}^n\frac{1}{\lambda_i(\mathcal{L}_R)}\right)\right).\end{aligned}$$

Remark 4. *The error bounds e^{droop} and e^ω can simultaneously be made arbitrarily small. However, the voltage error bound e^V is lower bounded by a constant. This is of course due to the necessity of a relative voltage drop for having a power flow between in an HVDC line.*

Proof: Consider the equilibrium of (6). Let $\hat{\omega}$ and $\hat{V}$ be defined by (7) – (8). By Assumption 1, we obtain the following expression

$$\begin{bmatrix}-(K^\omega+K^{\text{droop}}) & K^V\\ K^\omega & -(K^V+V^{\text{nom}}\mathcal{L}_R)\end{bmatrix}\begin{bmatrix}\hat{\omega}\\ \hat{V}\end{bmatrix}=\begin{bmatrix}-P^m\\ 0_{n\times 1}\end{bmatrix}. \tag{10}$$

By multiplying the last n rows of (10) with $\frac{k^\omega+k^{\text{droop}}}{k^\omega}$ and adding to the first n rows of (10), we obtain by Assumption 2

$$\underbrace{\left(\frac{(k^\omega+k^{\text{droop}})V^{\text{nom}}}{k^\omega}\mathcal{L}_R+\frac{k^{\text{droop}}k^V}{k^\omega}I_n\right)}_{\triangleq A_1}\hat{V}=P^m. \tag{11}$$

We write $\hat{V}=\sum_{i=1}^n a_i^1 v_i^1$, where v_i^1 is the ith eigenvector of A_1, with the corresponding eigenvalue λ_i^1. Note that the coefficients a_i^1 are unique, since A_1 is symmetric, implying that its eigenvectors form an orthonormal basis. Substituting the eigenvector decomposition of $\hat{V}$ in (11) yields

$$A_1\hat{V}=A_1\sum_{i=1}^n a_i^1 v_i^1=\sum_{i=1}^n\lambda_i^1 a_i^1 v_i^1=P^m,$$

which implies

$$a_i^1=\frac{(v_i^1)^T P^m}{\lambda_i^1}.$$

Let the eigenvalues be ordered by their increasing values. Clearly $\lambda_1^1 = \frac{k^{\text{droop}} k^V}{k^\omega}$ and $v_1^1 = \frac{1}{\sqrt{n}} 1_{n\times 1}$. This implies

$$\hat{V} = \frac{k^\omega 1_{1\times n} P^m}{n k^{\text{droop}} k^V} 1_{n\times 1} + \sum_{i=2}^{n} \frac{(v_i^1)^T P^m}{\lambda_i^1} v_i^1. \tag{12}$$

By noting that

$$\begin{aligned} \lambda_i^1 &= \frac{(k^\omega + k^{\text{droop}}) V^{\text{nom}} \lambda_i(\mathcal{L}_R) + k^{\text{droop}} k^V}{k^\omega} \\ &\geq \frac{(k^\omega + k^{\text{droop}}) V^{\text{nom}} \lambda_i(\mathcal{L}_R)}{k^\omega}, \end{aligned} \tag{13}$$

where $\lambda_i(\mathcal{L}_R)$ is the ith eigenvalue of $\mathcal{L}_R$, we obtain the following bound on $\hat{V}$

$$\begin{aligned} \left\| \hat{V} \right\|_\infty &\leq \frac{k^\omega \left| 1_{1\times n} P^m \right|}{n k^{\text{droop}} k^V} + \frac{\max_i \left| P_i^m \right| k^\omega}{(k^\omega + k^{\text{droop}}) V^{\text{nom}}} \sum_{i=2}^{n} \frac{1}{\lambda_i(\mathcal{L}_R)} \\ &\leq \frac{k^\omega \left| \sum_{i=1}^n P_i^m \right|}{n k^{\text{droop}} k^V} + \frac{\max_i \left| P_i^m \right|}{V^{\text{nom}}} \sum_{i=2}^{n} \frac{1}{\lambda_i(\mathcal{L}_R)}. \end{aligned}$$

From the first n rows of (10), and by substituting the expression for $\hat{V}$ from (12), we have

$$\begin{aligned} \hat{\omega} &= \frac{k^V \hat{V} - P^m}{k^\omega + k^{\text{droop}}} \\ &= \frac{1}{k^\omega + k^{\text{droop}}} \left(- \frac{k^\omega 1_{1\times n} P^m}{n k^{\text{droop}}} 1_{n\times 1} \right. \\ &\quad \left. + \sum_{i=2}^{n} \frac{k^V (v_i^1)^T P^m}{\lambda_i^1} v_i^1 - P^m \right). \end{aligned} \tag{14}$$

By using the bound on λ_i^1 from (13), we obtain

$$\begin{aligned} \|\hat{\omega}\|_\infty \leq \frac{1}{k^{\text{droop}}} \left(\frac{\left| \sum_{i=1}^n P_i^m \right|}{n} \right. \\ \left. + \max_i P_i^m \left(1 + \frac{k^V}{V^{\text{nom}}} \sum_{i=2}^{n} \frac{1}{\lambda_i(\mathcal{L}_R)} \right) \right). \end{aligned}$$

Consider now the power generated by the voltage droop controller. By (14) we obtain

$$\begin{aligned} P^{\text{droop}} + \frac{1}{n} \sum_{i=1}^{n} P_i^m 1_{n\times 1} &= k^{\text{droop}} \hat{\omega} + \frac{1_{1\times n} P^m}{n} 1_{n\times 1} \\ &= \frac{k^{\text{droop}}}{k^\omega + k^{\text{droop}}} \left(- \frac{1}{n} \sum_{i=1}^{n} P_i^m 1_{n\times 1} - P^m \right. \\ &\quad \left. + \sum_{i=2}^{n} \frac{k^V (v_i^1)^T P^m}{\lambda_i^1} v_i^1 \right). \end{aligned}$$

By using the bound on λ_i^1 in (13), we obtain

$$\begin{aligned} \left\| P^{\text{droop}} + \frac{1}{n} \sum_{i=1}^{n} P_i^m 1_{n\times 1} \right\|_\infty &\leq \frac{k^{\text{droop}}}{k^\omega + k^{\text{droop}}} \left(\frac{1}{n} \left| \sum_{i=1}^{n} P_i^m \right| \right. \\ &\quad \left. + \max_i |P_i^m| \left(1 + \sum_{i=2}^{n} \frac{k^\omega}{(k^\omega + k^{\text{droop}}) V^{\text{nom}} \lambda_i(\mathcal{L}_R)} \right) \right) \\ &\leq \frac{k^{\text{droop}}}{k^\omega + k^{\text{droop}}} \left(\frac{1}{n} \left| \sum_{i=1}^{n} P_i^m \right| \right. \\ &\quad \left. + \max_i |P_i^m| \left(1 + \frac{1}{V^{\text{nom}}} \sum_{i=2}^{n} \frac{1}{\lambda_i(\mathcal{L}_R)} \right) \right), \end{aligned}$$

which completes the proof. ■

VI. RL-line model for DC grids

In this section we extend the HVDC line model to consider the inductance of the HVDC lines. The voltage dynamics of the HVDC converter i are given by

$$C_i \dot{V}_i = - \sum_{j\in\mathcal{N}_i} I_{ij}, \tag{15}$$

while the current dynamics of the HVDC line (i,j), connecting converter i with converter j, are given by

$$L_{ij} \dot{I}_{ij} = -R_{ij} I_{ij} + V_i - V_j, \tag{16}$$

where L_{ij} is the inductance of line (i,j). This line model is illustrated in Figure 3. Denote by I_{ij}^{nom} the nominal current through line (i,j). Combining the voltage dynamics (15), the current dynamics (16), the frequency dynamics (2), the voltage controller (3) and the power-current relationship (5), we obtain the following closed-loop dynamics

$$\begin{aligned} \begin{bmatrix} \dot{\omega} \\ \dot{V} \\ \dot{I} \end{bmatrix} &= \begin{bmatrix} -M(K^\omega + K^{\text{droop}}) & MK^V & 0_{n\times m} \\ \frac{1}{V^{\text{nom}}} CK^\omega & -\frac{1}{V^{\text{nom}}} CK^V & -C\mathcal{B} \\ 0_{m\times n} & L\mathcal{B}^T & -LR \end{bmatrix} \begin{bmatrix} \omega \\ V \\ I \end{bmatrix} \\ &\quad + \begin{bmatrix} M\left((K^\omega + K^{\text{droop}}) \omega^{\text{ref}} 1_{n\times 1} - K^V V^{\text{ref}} \right) \\ C\left(\frac{1}{V^{\text{nom}}} K^V V^{\text{ref}} - \frac{\omega^{\text{ref}}}{V^{\text{nom}}} K^\omega 1_{n\times 1} \right) \\ 0_{m\times 1} \end{bmatrix} \\ &\quad + \begin{bmatrix} M(P^m + P^{\text{nom}} - P^{\text{inj, nom}}) \\ \frac{1}{V^{\text{nom}}} C P^{\text{inj, nom}} \\ 0_{m\times 1} \end{bmatrix}, \end{aligned} \tag{17}$$

where $I = [I_1, \ldots, I_m]^T$, $L = \text{diag}([L_1^{-1}, \ldots, L_m^{-1}])$ and $R = \text{diag}([R_1, \ldots, R_m])$, where m is the number of HVDC transmission lines, and $1, \ldots, m$ defines an ordering of the HVDC lines. Denote by $I^{\text{ref}} = [I_1^{\text{ref}}, \ldots, I_m^{\text{ref}}]^T$ the nominal currents of the HVDC lines.

Assumption 3. *The reference frequency, voltages and currents define an equilibrium of the closed loop system when there is no mechanical load. This implies that* $[\omega^T, V^T, I^T]^T = [\omega^{ref} 1_{1\times n}, (V^{ref})^T, (I^{ref})^T]^T$ *is an equilibrium of* (19)*, when* $P^m = 0_{n\times 1}$*. By substituting this in* (19)*,*

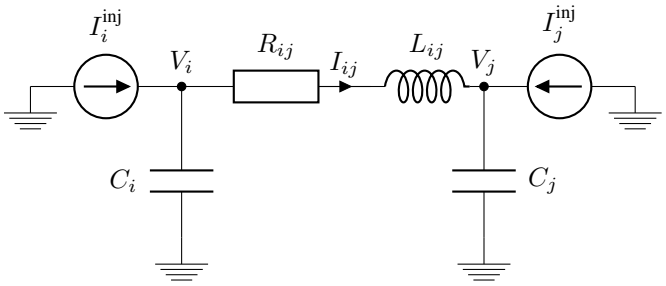

Figure 3. RL-line model of a transmission line.

we obtain that $P^{nom} = P^{inj,\ nom}$*, and* $\mathcal{B}I^{ref} = V^{nom}\mathcal{L}_R V^{ref} = P^{inj,\ nom} = P^{nom}$.

Let the incremental frequencies and voltages be defined by (7) and (8), respectively, and define

$$\hat{I} = I - I^{\text{ref}}. \tag{18}$$

This allows us to rewrite (19) as

$$\begin{bmatrix} \dot{\hat{\omega}} \\ \dot{\hat{V}} \\ \dot{\hat{I}} \end{bmatrix} = \begin{bmatrix} -M(K^{\omega} + K^{\text{droop}}) & MK^{V} & 0_{n\times m} \\ \frac{1}{V^{\text{nom}}} CK^{\omega} & -\frac{1}{V^{\text{nom}}} CK^{V} & -C\mathcal{B} \\ 0_{m\times n} & L\mathcal{B}^{T} & -LR \end{bmatrix} \begin{bmatrix} \hat{\omega} \\ \hat{V} \\ \hat{I} \end{bmatrix} + \begin{bmatrix} MP^{m} \\ 0_{n\times 1} \\ 0_{m\times 1} \end{bmatrix}. \tag{19}$$

We observe that the last m rows of (19) imply that the equilibrium satisfies $L\mathcal{B}^T\hat{V} = LR\hat{I}$. Premultiplying this relation with $\mathcal{B}R^{-1}L^{-1}$ yields $\mathcal{B}R^{-1}\mathcal{B}^T\hat{V} = \mathcal{L}\hat{V} = \mathcal{B}\hat{I}$. Thus, the equilibrium of (9) corresponds to $[\hat{\omega}^T, \hat{V}^T]^T$ of the equilibrium of (19). Hence, Theorem 2 holds also for the dynamics (19). Now we show that the dynamics of (19) are stable. By decomposing (19) into two subsystems, we obtain

$$\begin{cases} \dot{\hat{\omega}} = -M(K^{\text{droop}} + K^{\omega})\hat{\omega} + MK^{V}u_1 \\ y_1 = \frac{1}{V^{\text{nom}}} K^{\omega}\hat{\omega} \end{cases} \tag{S_1}$$

$$\begin{cases} \dot{\hat{V}} = -\frac{1}{V^{\text{nom}}} CK^{V}\hat{V} - C\mathcal{B}\hat{I} + Cu_2 \\ \dot{\hat{I}} = L\mathcal{B}^{T}\hat{V} - LR\hat{I} \\ y_2 = \hat{V}, \end{cases} \tag{S_2'}$$

where (S_1) and (S_2') are interconnected through $u_1 = y_2 + (K^V)^{-1}P^m, u_2 = y_1$. By Proposition 1, (S_1) is strictly passive. We proceed to show that (S_2') is strictly passive.

Proposition 1. *The system* (S_2') *is strictly passive.*

Proof: Consider the storage function

$$W_2' = \frac{1}{2}\hat{V}^T C^{-1}\hat{V} + \frac{1}{2}\hat{I}^T L^{-1}\hat{I}.$$

Differentiating W_2' with respect to time along trajectories of (S_2') yields

$$\begin{aligned} \dot{W}_2' &= \hat{V}^T C^{-1}\dot{\hat{V}} + \hat{I}^T L^{-1}\dot{\hat{I}} \\ &= \hat{V}^T C^{-1}\left(-\frac{1}{V^{\text{nom}}} CK^{V}\hat{V} - C\mathcal{B}\hat{I} + Cu_2\right) \\ &\quad + \hat{I}^T L^{-1}\left(L\mathcal{B}^T\hat{V} - LR\hat{I}\right) \\ &= -\frac{\hat{V}^T K^{V}\hat{V}}{V^{\text{nom}}} - \hat{V}^T\mathcal{B}\hat{I} + \hat{V}^T u_2 + \hat{I}^T\mathcal{B}^T\hat{V} - \hat{I}^T R\hat{I} \\ &= -\frac{\hat{V}^T K^{V}\hat{V}}{V^{\text{nom}}} - \hat{I}^T R\hat{I} + y_2^T u_2 \end{aligned}$$

which shows that (S_2') is strictly passive. ■

Theorem 3. *The system defined by* (19) *is globally asymptotically stable.*

Proof: The interconnection of any two strictly passive systems is asymptotically stable [12]. Since the storage functions W_1 and W_2' are radially unbounded, the stability of (9) is global. ■

VII. Simulations

In this section, we simulate the proposed controller on an MTDC grid connecting three asynchronous AC areas, whose main purpose is bulk power transfer between the AC areas. The test grid consists of tree 6 bus AC grids, described in detail in [21], connected with a 3 bus MTDC grid. In Figure 4, the topology of the interconnected MTDC-AC grid is shown.

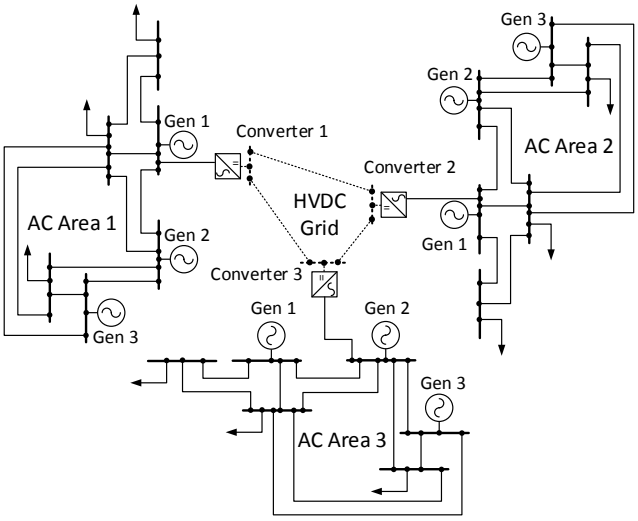

Figure 4. Test grid consisting of 3 AC areas, connected by an MTDC grid consisting of 3 converter stations and 3 DC lines.

Each converter station is controlled with (3). While the converter dynamics are ignored due to their fast nature, the nonlinear relation (4) is used to relate the injected AC powers with the HVDC currents. The physical system parameters and the controller parameters are given in Table I, II, respectively. The simulation was conducted by using an extended version of MatDyn [6], taking also the HVDC dynamics into account. The simulation starts in steady-state,

Table I
HVDC GRID LINE PARAMETERS

From	To	Resistance [p.u.]	Reactance [p.u.]
1	2	0.0015	0.01
1	3	0.0045	0.03
2	3	0.0015	0.01

Table II
CONTROLLER PARAMETER

K_1^{ω}	K_2^{ω}	K_3^{ω}	K_1^{droop}	K_2^{droop}	K_3^{droop}
501	501	501	667	667	667

and at time 1 s an immediate change in load from 0.7 p.u. (per-unit) to 0.8 p.u. occurs at bus 4 in the AC area 1. The local frequency controllers at the generators will react immediately to the resulting frequency drop, and start to accelerate. The frequencies of the generators are shown in Figure 5.

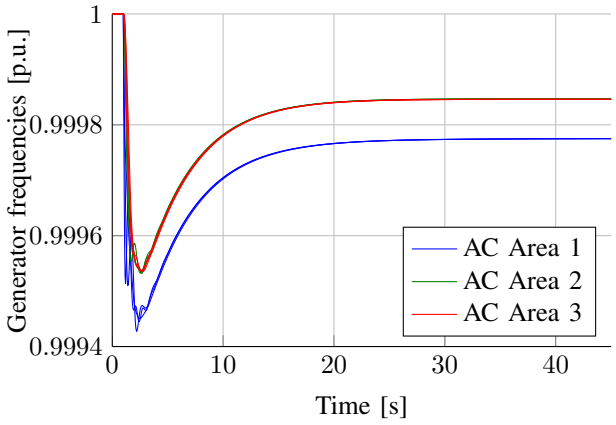

Figure 5. Frequencies of the generator areas.

After a few second all generator frequencies within the same AC area synchronize, and after about 30 s the frequencies converge to the new equilibrium. The frequency deviation is larger in AC area 1 than in the remaining AC areas, but the differences are rather small, in accordance with Theorem 2. Figure 6 shows the changes in the power output of the generators. The disturbance is shared along all generators. The injected powers through the converter are shown in Figure 7. Since the converter dynamics are much faster than the AC systems, they are neglected in the simulation and it is assumed that the converter power tracks the controller output perfectly. Due to the increased load, the DC voltages of all converters increase, see Figure 8. However, as predicted by Theorem 2, both the absolute and relative voltage deviations are bounded.

VIII. DISCUSSION AND CONCLUSIONS

In this paper we have proposed a decentralized proportional controller for sharing primary frequency control reserves in asynchronous AC systems connected through an

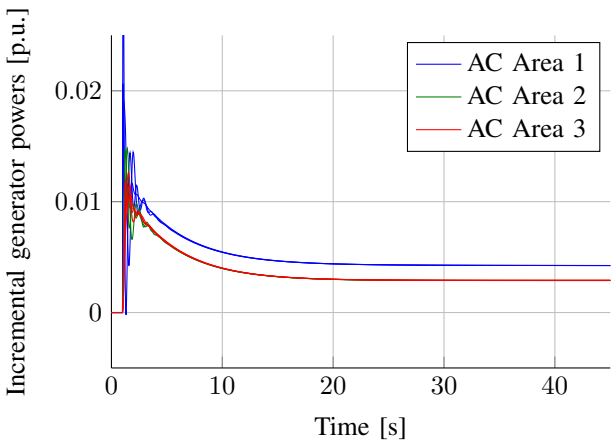

Figure 6. Incremental generator power levels.

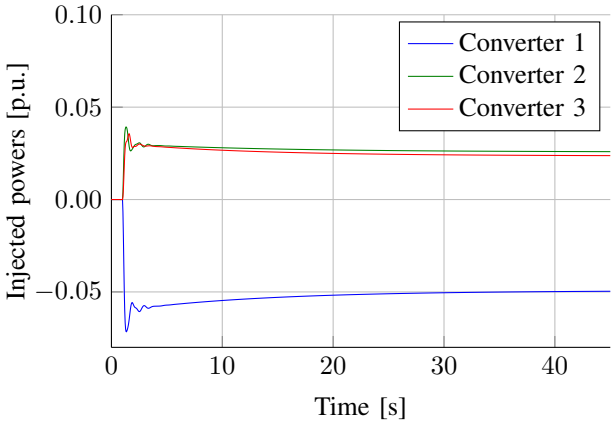

Figure 7. Injected power levels at the converters.

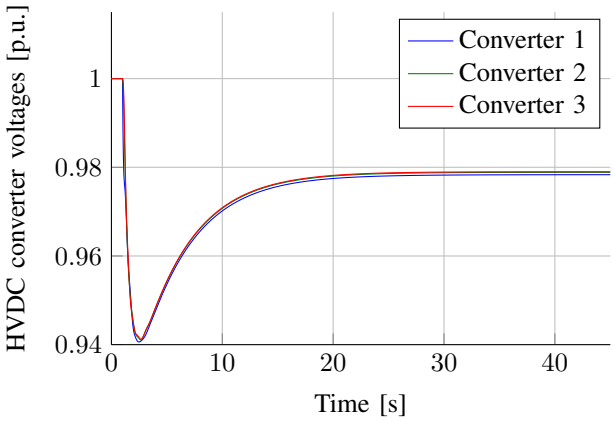

Figure 8. Voltages of the DC converters.

MTDC system. The controller uses the local frequency in the AC grid and the local DC voltage as inputs in order to control the power injections into the MTDC grid. The resulting closed-loop system is shown to be globally stable regardless of the controller parameters by passivity arguments. It is also shown that the DC voltages and AC frequencies at the equilibrium are close to their nominal values. Furthermore

the generated power from the primary frequency control is approximately shared fairly between the AC areas. The deviation from perfectly fair power sharing is quantified. The proposed controller was simulated on a test system consisting of 3 AC areas combined with an MTDC grid to demonstrate its effectiveness. The paper constitutes a first step towards utilizing the increased flexibility which future MTDC grids will provide to the connected AC systems. Future work will focus on extending the primary proportional controller with secondary controllers, where communication and integral action will be necessary to eliminate static control errors. An extensive simulation study on more realistic grid topologies and dynamical models is also ongoing work.

REFERENCES

[1] M. Andreasson, D. V. Dimarogonas, H. Sandberg, and K. H. Johansson. Control of mtdc transmission systems under local information. In *IEEE Conference on Decision and Control*, Dec. 2014.

[2] M. Andreasson, M. Nazari, D. V. Dimarogonas, H Sandberg, K. H. Johansson, and M. Ghandhari. Distributed voltage and current control of multi-terminal high-voltage direct current transmission systems. In *IFAC World Congress*, Aug. 2014.

[3] U. Axelsson, A. Holm, C. Liljegren, M. Aberg, K. Eriksson, and O. Tollerz. The gotland HVDC light project-experiences from trial and commercial operation. In *Electricity Distribution, 2001. Part 1: Contributions. CIRED. 16th International Conference and Exhibition on (IEE Conf. Publ No. 482)*, volume 1, pages 5–pp. IET, 2001.

[4] P. Bresesti, W.L. Kling, R.L. Hendriks, and R. Vailati. HVDC connection of offshore wind farms to the transmission system. *Energy Conversion, IEEE Transactions on*, 22(1):37–43, March 2007.

[5] M. Callavik, A. Blomberg, J. Häfner, and B. Jacobson. The hybrid HVDC breaker. *ABB Grid Systems, Technical Paper*, 2012.

[6] S. Cole and R. Belmans. Matdyn, a new matlab based toolbox for power system dynamic simulation. *Power Systems, IEEE Transactions on*, 26(3):1129–1136, Aug 2011.

[7] J. Dai and G. Damm. An improved control law using HVDC systems for frequency control. In *Proc. 17th power systems computation conf*, 2011.

[8] J. Dai, Y. Phulpin, A. Sarlette, and D. Ernst. Impact of delays on a consensus-based primary frequency control scheme for AC systems connected by a multi-terminal HVDC grid. In *Bulk Power System Dynamics and Control (iREP)-VIII (iREP), 2010 iREP Symposium*, pages 1–9. IEEE, 2010.

[9] J. Dai, Y. Phulpin, A. Sarlette, and D. Ernst. Voltage control in an HVDC system to share primary frequency reserves between non-synchronous areas. In *Proc. 17th power systems computation conf*, 2011.

[10] C.M. Franck. HVDC circuit breakers: A review identifying future research needs. *Power Delivery, IEEE Transactions on*, 26(2):998–1007, April 2011.

[11] T.M. Haileselassie and K. Uhlen. Power system security in a meshed north sea HVDC grid. *Proceedings of the IEEE*, 101(4):978–990, April 2013.

[12] H.K. Khalil. *Nonlinear Systems*. Prentice Hall, 2002.

[13] R. Li, S. Bozhko, and G. Asher. Frequency control design for offshore wind farm grid with lcc-HVDC link connection. *Power Electronics, IEEE Transactions on*, 23(3):1085–1092, 2008.

[14] J. Machowski, J. W. Bialek, and J. R. Bumby. *Power System Dynamics: Stability and Control*. Wiley, 2008.

[15] Z. Melhem. *Electricity Transmission, Distribution and Storage Systems*. Woodhead Publishing Series in Energy. Elsevier Science, 2013.

[16] K.R. Padiyar. *HVDC power transmission systems: technology and system interactions*. New Age International, 1990.

[17] B. Silva, C. L. Moreira, L. Seca, Y. Phulpin, and J. A. Peas Lopes. Provision of inertial and primary frequency control services using offshore multiterminal HVDC networks. *Sustainable Energy, IEEE Transactions on*, 3(4):800–808, 2012.

[18] D. Van Hertem, M. Ghandhari, and M. Delimar. Technical limitations towards a SuperGrid - A European prospective. In *IEEE International Energy Conference and Exhibition (EnergyCon)*, pages 302 –309, dec. 2010.

[19] R. Wiget and G. Andersson. Optimal power flow for combined AC and multi-terminal HVDC grids based on vsc converters. In *IEEE Power and Energy Society General Meeting, San Diego, USA*, pages 1–8, 2012.

[20] J. C. Willems. Dissipative dynamical systems part i: General theory. *Archive for rational mechanics and analysis*, 45(5):321–351, 1972.

[21] A.J.W.B. Wollenberg. *Power generation operation & control, 2nd ed (With CD)*. Wiley India Pvt. Limited, 2006.